Article

Not peer-reviewed version

Non-Linear Quantum Dynamics in Coupled Double-Quantum-Dot-Cavity Systems

Tatiana Mihaescu , Mihai A. Macovei , Aurelian Isar *

Posted Date: 19 August 2025

doi: 10.20944/preprints202508.1322.v1

Keywords: double quantum dot; microwave cavity; inter-dot Coulomb interaction; two-photon resonance; photon statistics

Article

Non-Linear Quantum Dynamics in Coupled Double-Quantum-Dot-Cavity Systems

Tatiana Mihaescu [1], Mihai A. Macovei [2] and Aurelian Isar [1,*]

[1] National Institute of Physics and Nuclear Engineering, 30 Reactorului, POB-MG6, Bucharest-Magurele, Romania
[2] Institute of Applied Physics, Moldova State University, Academiei str. 5, MD-2028 Chişinău, Moldova
* Correspondence: isar@theory.nipne.ro

Abstract

The steady-state quantum dynamics of a compound sample consisting of a semiconductor double quantum dot (DQD) system, non-linearly coupled with a leaking superconducting transmission line resonator, is theoretically investigated. Particularly, the transition frequency of the DQD is taken equal to the doubled resonator frequency, whereas the inter-dot Coulomb interaction is being considered weak. As a consequence, the steady-state quantum dynamics of this complex non-linear system exhibits sudden changes of its features, occuring at a critical DQD-cavity coupling strength, respectively. We have shown that above the threshold, the electrical current through the double quantum dot follows the mean photon number into the microwave mode inside the resonator. This might not be the case anymore below that critical coupling strength. Furthermore, the photon quantum correlations vary from super-Poissonian to Poissonian photon statistics, i.e. towards single-qubit lasing phenomena at microwave frequencies.

Keywords: double quantum dot; microwave cavity; inter-dot Coulomb interaction; two-photon resonance; photon statistics

---

Dedication to Professor Viktor Dodonov for his 55 Years in Quantum Physics

1. Introduction

The various examples of hybrid circuit quantum electrodynamics (QED) structures exhibit a variety of quantum effects previously achieved mainly in the quantum optical setups, while presenting unquestionable advantage in the form of low-size on-chip implementation [1–5]. An emblematic example is the optical cavity coupling natural atoms and photons, where also lasing phenomena are accomplished by additionally optically pumping the atom. A successful QED alternative system playing the role of the active medium that may induce light amplification in the resonant cavity are the artificial atoms, i.e. semiconducting double quantum dots (DQDs) attached to normal metal leads assuring the pumping via applied biased voltage [6–9]. The circuit considered is driven by single-electron tunneling leading to a population inversion in the DQD energy levels such that, in the resonance condition with the cavity, the electron transport takes place via the emission of energy quantum into the cavity [10–12]. In consequence, also the excited microwave oscillator in the cavity may facilitate the current flow in the DQD [13,14].

The advantage of studying DQD-microwave resonator systems is twofold. First of all, the semiconducting DQDs are perfect candidates for qubits due to their higher degree of tunability and to the experimentally attainable strong-coupling regime with the electromagnetic cavity demonstrated in Refs. [15–18]. Secondly, DQDs are very efficient detectors of single itinerant microwave photons, which is a desirable trait of a quantum system for the realisation of quantum information processing tasks [19,20]. Needless to say that an electronic interface for the manipulation of the photon statistics represents a promising environment for the implementation of various applications in nano-device technology [4,10,21].

The DQDs coupled to a leaking resonator and immersed in various environments still show unexplored physics fueling an increasing theoretical interest and further investigations [14,20,22–27]. Also different practical configurations may include weak Coulomb interaction between the charges [28–32], Kerr nonlinearity and signal driven cavity or DQD [14,33–36]. Thus, numerous theoretical inquiries demonstrate the control of photon emission via transport properties in the DQD and a variety of lasing resonances and their signatures in the transport current [28,37–41]. In addition, the Markovian master equation approach is applied which incorporates the dissipation and decoherence processes deteriorating the performance of the device due to the interaction with the degrees of freedom of the electronic and bosonic baths [42,43].

In this work we analyse the quantum dynamics of a complex system formed of a leaking superconducting transmission line resonator mode coupled with a semiconductor DQD qubit, while focusing on the two-photon resonance between the cavity mode and the energy separation levels of the DQD. Additionally, the interdot Coulomb interaction is considered weak, allowing for the simultaneous presence of two electrons in DQD, but only one in each dot. Compared to the strong Coulomb interaction, under the two photon resonance condition covered recently [44,45], in the current study an additional incoherent electronic tunneling channel is established, contributing to the population of the DQD and facilitating stronger lasing effects in the resonator as a result. In the framework of open quantum systems we employ the master equation for this system configuration and deduce the photon number characteristics and the average electronic current in the asymptotic limit of the steady state. We have found a critical value for the qubit-cavity coupling strengths such that the mean-number of the cavity photons substantially enhances or suppresses, and so does the electric current through the DQD sample. This suggests a convenient conversion mechanism of electric current into a microwave photon flux, or reciprocally. Furthermore, above threshold the electrical current through the double quantum dot follows the behaviours of mean photon numbers into the microwave mode inside the resonator, while this might not be the case below that critical point. Finally, the photon correlations vary from super-Poissonian to Poissonian photon statistics, that is, towards single-qubit lasing effects at microwave frequencies.

This paper is organized as follows. In Sec. 2 we describe the analytical approach and the system of interest, while in Sec. 3 we present the equations of motion characterising the considered system. Sec. 4 presents and analyses the obtained results. The article concludes with a summary given in Sec. 5.

2. Analytical Approach

We consider a hybrid setup made of a semiconducting DQD qubit which is coupled to an electromagnetic microwave resonator such as a superconducting transmission line. Furthermore, the DQD system is pumped incoherently via electron tunneling through the dots, by means of the bias voltage that is assumed to be high. The Coulomb interaction is considered weak, meaning that the DQD is described by the following possible states, see e.g. Ref. [28]: the null-electron subspace or the empty-dot state, i.e. $|o\rangle$, together with the single-electron subspaces, where the electron is localized either on the left, $|L\rangle$, or the right dot, $|R\rangle$, respectively, as well as the mixed state $|LR\rangle$ denoting the situation when simultaneously two electrons are localised separately in each of the two quantum dots, with $|o\rangle\langle o| + |L\rangle\langle L| + |R\rangle\langle R| + |LR\rangle\langle RL| = 1$.

Assuming that the corresponding resonator as well as the DQD interaction with the photon or electronic environmental reservoirs are weak, in the Born-Markov approximations and low temperatures limit [22,28,44–47], one obtains the following master equation for the reduced density matrix ρ describing the qubit plus leaking resonator mode subsystem only, i.e.,

$$\frac{d}{dt}\rho(t) + \frac{i}{\hbar}[H,\rho] = \Lambda_L\rho + \Lambda_R\rho + \Lambda_c\rho, \tag{1}$$

where the entire Hamiltonian, describing the investigated system, is given by

$$H = H_q + H_r. \tag{2}$$

Here, see e.g. [22,28],

$$H_q = \frac{\hbar\epsilon}{2}\sigma_z + \hbar\tau(\sigma^+ + \sigma^-) + \hbar u|m\rangle\langle m| \tag{3}$$

is the Hamiltonian of two quantum dots, forming the DQD qubit, with ϵ being their energy separation, while τ is the inter-dot tunnelling amplitude, whereas u denotes the inter-dot Coulomb interaction and $|m\rangle \equiv |LR\rangle$. The Hamiltonian

$$H_r = \hbar\omega_r a^\dagger a + \hbar g\sigma_z(a^\dagger + a) \tag{4}$$

describes the microwave resonator free energy and qubit-cavity interaction, respectively, with ω_r and g being the corresponding resonator frequency and coupling strength. The cavity photon creation (annihilation) operators, $a^\dagger(a)$, obey the standard commutation relations: $[a, a^\dagger] = 1$, $[a, a] = [a^\dagger, a^\dagger] = 0$. On the other side, the qubit operators are defined as follows: $\sigma_z = |L\rangle\langle L| - |R\rangle\langle R|$, $\sigma^+ = |L\rangle\langle R|$ and $\sigma^- = |R\rangle\langle L|$, which obey the commutation relations for su(2) algebra, that is, $[\sigma^+, \sigma^-] = \sigma_z$ and $[\sigma_z, \sigma^\pm] = \pm 2\sigma^\pm$. The damping terms, entering in the right-side part of the master equation (1), are represented as follows:

$$\begin{aligned}
\Lambda_L\rho &= -\frac{\Gamma_L}{2}[s_L, s_L^+\rho] + H.c.,\\
\Lambda_R\rho &= -\frac{\Gamma_R}{2}[s_R^+, s_R\rho] + H.c.,\\
\Lambda_c\rho &= -\frac{\kappa}{2}[a^\dagger, a\rho] + H.c.,
\end{aligned} \tag{5}$$

where Γ_L, Γ_R and κ are the corresponding electron tunneling rates and the cavity decay rate, while [28]: $s_L = |o\rangle\langle L| + |R\rangle\langle m|$ and $s_R = |o\rangle\langle R| - |L\rangle\langle m|$.

Diagonalizing the first two terms of the Hamiltonian (3), using the transformation

$$\begin{aligned}
|L\rangle &= \cos(\theta/2)|e\rangle - \sin(\theta/2)|g\rangle,\\
|R\rangle &= \sin(\theta/2)|e\rangle + \cos(\theta/2)|g\rangle,
\end{aligned} \tag{6}$$

with $\cos\theta = \epsilon/\Omega$, $\sin\theta = 2\tau/\Omega$ and $\Omega = \sqrt{\epsilon^2 + (2\tau)^2}$, one arrives at a Hamiltonian H represented via new qubit quasispin operators, namely, $R_{\alpha\beta} = |\alpha\rangle\langle\beta|$, $\{\alpha, \beta \in o, e, g, m\}$, satisfying the commutation relations: $[R_{\alpha\beta}, R_{\beta'\alpha'}] = \delta_{\beta\beta'}R_{\alpha\alpha'} - \delta_{\alpha'\alpha}R_{\beta'\beta}$, that is,

$$\begin{aligned}
H &= \hbar\Omega R_z/2 + \hbar\omega_r a^\dagger a + \hbar u|m\rangle\langle m| + \hbar g\big(\cos\theta R_z\\
&- \sin\theta(R_{eg} + R_{ge})\big)\big(a + a^\dagger\big),
\end{aligned} \tag{7}$$

with $R_z = |e\rangle\langle e| - |g\rangle\langle g|$ being the inversion operator.

In the following we assume that the semiconductor DQD exchanges energy with the resonator mode when its generalized frequency Ω is equal approximately to the doubled value of the cavity frequency ω_r. Then in the interaction picture, given by the unitary operator $U(t) = \exp(iH_0 t/\hbar)$ with $H_0 = \hbar\Omega R_z/2 + \hbar\omega_r a^\dagger a$, we will arrive at a time-dependent Hamiltonian, $H_f(t)$, oscillating fastly in time. Its contribution to the established quantum dynamics can be obtained via the relation:

$$\bar{H} = -\frac{i}{\hbar}H_f(t)\int dt H_f(t), \tag{8}$$

when $g \ll \omega_r$, see e.g. [48,49]. As a result, the master equation (1) transforms as:

$$\begin{aligned}
\frac{d}{dt}\rho(t) &+ \frac{i}{\hbar}[\bar{H},\rho] = -\Gamma_{Lc}[R_{oe}+R_{gm},(R_{eo}+R_{mg})\rho] \\
&- \Gamma_{Ls}[R_{og}-R_{em},(R_{go}-R_{me})\rho] \\
&- \Gamma_{Rs}[R_{eo}+R_{mg},(R_{oe}+R_{gm})\rho] \\
&- \Gamma_{Rc}[R_{go}-R_{me},(R_{og}-R_{em})\rho] \\
&- \frac{\kappa}{2}[a^{\dagger},a\rho]+H.c., \qquad (9)
\end{aligned}$$

where

$$\begin{aligned}
\bar{H} &= \hbar\omega_e R_{ee} - \hbar\omega_g R_{gg} + \hbar\delta a^{\dagger}a + \hbar u|m\rangle\langle m| + \hbar\beta R_z a^{\dagger}a \\
&+ \hbar\bar{g}(a^{\dagger 2}R_{ge} + R_{eg}a^2). \qquad (10)
\end{aligned}$$

Here $\omega_e = \beta/2 - \omega_s$, $\omega_g = \beta/2 + \omega_s$, $\beta = 2g^2\Omega\sin^2\theta/(\Omega^2-\omega_r^2)$, $\omega_s = g^2(\Omega^2\cos^2\theta - \omega_r^2)/[\omega_r(\Omega^2-\omega_r^2)]$, $\delta = \omega_r - \Omega/2$ and $\bar{g} = g^2\Omega\sin 2\theta/[2\omega_r(\Omega-\omega_r)]$. The corresponding rates are:

$$\begin{aligned}
\Gamma_{Lc} &= \Gamma_L\cos^2(\theta/2)/2, \;\; \Gamma_{Ls} = \Gamma_L\sin^2(\theta/2)/2, \\
\Gamma_{Rc} &= \Gamma_R\cos^2(\theta/2)/2, \;\; \Gamma_{Rs} = \Gamma_R\sin^2(\theta/2)/2.
\end{aligned}$$

Notice that the master equation (9) was obtained under the secular approximation, i.e., we have considered that $\Omega \pm u \gg \Gamma_{L/R}$.

In the following Section we shall make use of Eq. (9) in order to obtain the corresponding equations of motion describing the quantum dynamics of the combined resonator-DQD subsystem.

3. The Equations of Motion

Using the master equation (9), one can obtain the following exact system of equations of motion describing the entire sample incorporating a semiconductor DQD qubit coupled respectively in two-photon resonance to the cavity boson-mode, i.e.,

$$\begin{aligned}
\dot{P}_n^{(0)} &= -\Gamma_L P_n^{(0)} + 2\Gamma_{Rs}P_n^{(3)} + 2\Gamma_{Rc}P_n^{(1)} - \kappa\big(nP_n^{(0)} \\
&- (n+1)P_{n+1}^{(0)}\big), \\
\dot{P}_n^{(1)} &= -i\bar{g}P_n^{(6)} - 2(\Gamma_{Lc}+\Gamma_{Rc})P_n^{(1)} + 2\Gamma_{Ls}P_n^{(0)} \\
&+ 2\Gamma_{Rs}P_n^{(2)} - \kappa\big(nP_n^{(1)} - (n+1)P_{n+1}^{(1)}\big), \\
\dot{P}_n^{(2)} &= -\Gamma_R P_n^{(2)} + 2\Gamma_{Lc}P_n^{(1)} + 2\Gamma_{Ls}P_n^{(3)} - \kappa\big(nP_n^{(2)} \\
&- (n+1)P_{n+1}^{(2)}\big), \\
\dot{P}_n^{(3)} &= -i\bar{g}P_n^{(4)} - 2(\Gamma_{Ls}+\Gamma_{Rs})P_n^{(3)} + 2\Gamma_{Lc}P_n^{(0)} \\
&+ 2\Gamma_{Rc}P_n^{(2)} - \kappa\big(nP_n^{(3)} - (n+1)P_{n+1}^{(3)}\big), \\
\dot{P}_n^{(4)} &= i\big((3+2n)\beta - 2\delta\big)P_n^{(5)} - 2i\bar{g}(n+1)(n+2) \\
&\times \big(P_n^{(3)} - P_{n+2}^{(1)}\big) - (\Gamma+\kappa)P_n^{(4)} - \kappa\big(nP_n^{(4)} \\
&- (n+1)P_{n+1}^{(4)}\big), \\
\dot{P}_n^{(5)} &= i\big((3+2n)\beta - 2\delta\big)P_n^{(4)} - (\Gamma+\kappa)P_n^{(5)} - \kappa\big(nP_n^{(5)} \\
&- (n+1)P_{n+1}^{(5)}\big),
\end{aligned}$$

$$
\begin{aligned}
\dot{P}_n^{(6)} &= i\big((1-2n)\beta+2\delta\big)P_n^{(7)} - 2i\bar{g}n(n-1)\big(P_n^{(1)}-P_{n-2}^{(3)}\big) \\
&- (\Gamma-\kappa)P_n^{(6)} - \kappa\big(nP_n^{(6)} - (n+1)P_{n+1}^{(6)} + 2P_n^{(8)}\big), \\
\dot{P}_n^{(7)} &= i\big((1-2n)\beta+2\delta\big)P_n^{(6)} - (\Gamma-\kappa)P_n^{(7)} - \kappa\big(nP_n^{(7)} \\
&- (n+1)P_{n+1}^{(7)} + 2P_n^{(9)}\big), \\
\dot{P}_n^{(8)} &= -i\big((1+2n)\beta-2\delta\big)P_n^{(9)} - 2i\bar{g}n(n+1)\big(P_{n+1}^{(1)}-P_{n-1}^{(3)}\big) \\
&- \Gamma P_n^{(8)} - \kappa\big(nP_n^{(8)} - (n+1)P_{n+1}^{(8)} - P_n^{(4)}\big), \\
\dot{P}_n^{(9)} &= -i\big((1+2n)\beta-2\delta\big)P_n^{(8)} - \Gamma P_n^{(9)} - \kappa\big(nP_n^{(9)} \\
&- (n+1)P_{n+1}^{(9)} + P_n^{(5)}\big). \qquad (11)
\end{aligned}
$$

The system of equations (11) can be easily obtained using the master equation (9), if one first gets the equations of motion for $\rho_{\alpha\beta}$=$\langle\alpha|\rho|\beta\rangle$, $\alpha,\beta \in \{o,e,g,m\}$, see also Refs. [50,51], and then writing the corresponding equations for the following variables: $\rho^{(0)} = \rho_{oo}$, $\rho^{(1)} = \rho_{gg}$, $\rho^{(2)} = \rho_{mm}$, $\rho^{(3)} = \rho_{ee}$, $\rho^{(4)} = a^2\rho_{ge} - \rho_{eg}a^{\dagger 2}$, $\rho^{(5)} = a^2\rho_{ge} + \rho_{eg}a^{\dagger 2}$, $\rho^{(6)} = a^{\dagger 2}\rho_{eg} - \rho_{ge}a^2$, $\rho^{(7)} = a^{\dagger 2}\rho_{eg} + \rho_{ge}a^2$, $\rho^{(8)} = a^{\dagger}\rho_{eg}a^{\dagger} - a\rho_{ge}a$ and $\rho^{(9)} = a^{\dagger}\rho_{eg}a^{\dagger} + a\rho_{ge}a$. The projection on the Fock states $|n\rangle$, i.e. $P_n^{(j)} = \langle n|\rho^{(j)}|n\rangle$, with $j \in \{0,\cdots,9\}$ and $n \in \{0,\infty\}$, will lead us to the system of equations (11), where $\Gamma = (\Gamma_L + \Gamma_R)/2$.

Generally, to solve the infinite system of equations (11), one truncates it at a certain maximum value $n = n_{max}$ so that a further increase in its value, i.e. n_{max}, does not modify the obtained results. As a consequence, the steady-state cavity-mode photon mean number, i.e. $\langle n\rangle = \langle a^{\dagger}a\rangle$, is expressed as:

$$
\langle n\rangle = \sum_{n=0}^{n_{max}} n\big(P_n^{(0)} + P_n^{(1)} + P_n^{(2)} + P_n^{(3)}\big), \qquad (12)
$$

with

$$
\sum_{n=0}^{n_{max}} \big(P_n^{(0)} + P_n^{(1)} + P_n^{(2)} + P_n^{(3)}\big) = 1.
$$

The current I_q through the DQD qubit is proportional to the population in the state $|R\rangle$ and $|m\rangle$, that is,

$$
\begin{aligned}
I_q &= |e|\Gamma_R\big(|R\rangle\langle R| + |m\rangle\langle m|\big) \qquad (13) \\
&= |e|\Gamma_R \sum_{n=0}^{n_{max}} \big(\cos^2(\theta/2)P_n^{(1)} + P_n^{(2)} + \sin^2(\theta/2)P_n^{(3)}\big),
\end{aligned}
$$

where e is the electron charge. In Exp. (13) we have applied the transformation (6) and the secular approximation.

The corresponding steady-state second-order cavity photon correlation function is defined in the usual way [52], namely,

$$
\begin{aligned}
g^{(2)}(0) &= \frac{\langle a^{\dagger 2}a^2\rangle}{\langle n\rangle^2} \qquad (14) \\
&= \frac{1}{\langle n\rangle^2}\sum_{n=0}^{n_{max}} n(n-1)\big(P_n^{(0)} + P_n^{(1)} + P_n^{(2)} + P_n^{(3)}\big).
\end{aligned}
$$

Note that $g^{(2)}(0) < 1$ means sub-Poissonian, $g^{(2)}(0) > 1$ super-Poissonian, and $g^{(2)}(0) = 1$ Poissonian photon statistics.

In the following Section we shall describe the photon resonator quantum dynamics, as well as the steady-state behaviours of the electrical current, based on results obtained from Eqs. (11-14).

4. Results and Discussion

Figure 1(a) shows the steady-state dependence of the mean cavity photon number as a function of the DQD-resonator coupling strength, near two-photon resonance, i.e. $\Omega \approx 2\omega_r$, extracted from the system of equations (11). Particularly, the decay rates were selected within the secular approximation, that is, smaller than qubit frequency Ω, in concordance with the valability of the master equation (9). As a result, we observe a threshold transition when the mean-photon number abruptly changes from lower to higher values, or conversely, by slightly varying the qubit-resonator coupling strength. Actually, this behaviour is typical for an externally coherently pumped and leaking cavity mode, containing a Kerr-like non-linearity [33,34], for instance. Here, however, this behaviour is due to the unilateral electronic pumping of the DQD sample, i.e. from the left to the right.

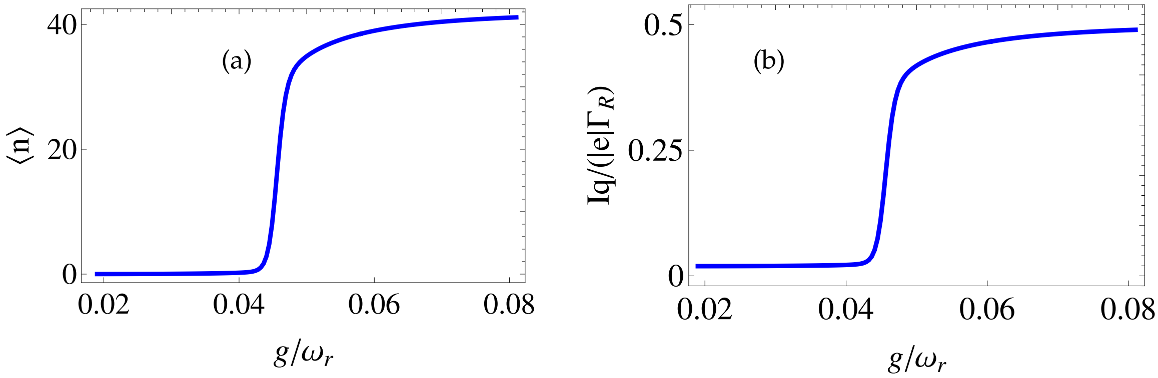

Figure 1. The steady-state behaviour of (a) the cavity mean photon number $\langle n\rangle = \langle a^\dagger a\rangle$ and (b) the steady-state dependence of the current I_q through the DQD system, as a function of g/ω_r. Here $\tau/\epsilon = 0.1$, $\epsilon/\omega_r = 1.96$, $\Gamma_L/\omega_r = \Gamma_R/\omega_r = 0.03$, $\kappa/\omega_r = 7\cdot 10^{-4}$.

On the other side, Figure 1(b) depicts the steady-state current through the DQD qubit, which is proportional to the populations in the state $|R\rangle$ and $|m\rangle$. It follows the same behaviour as the mean photon number, compare Figure 1(b) and Figure 1(a). Therefore, measuring the current through the DQD one can estimate the photon flux leaking out from the cavity mode, or vice versa. Practically, the described process is a useful tool to convert electric current into microwave photons in DQD-cavity systems. Moreover, the cavity photons obey the super-Poissonian statistics below the threshold, i.e. $g^{(2)}(0) \geq 2$, see Figure (2), which changes to Poissonian photons statistics above the threshold, i.e. to microwave photon lasing effects where $g^{(2)}(0) = 1$. Furthermore, around the threshold, the photon correlation evidently enhances. Also, $g^{(2)}(0)$ does not converge for $g/\omega_r = 0$, since $\langle n\rangle = 0$, so one should proceed with non-zero values for DQD-cavity coupling strengths in this particular case.

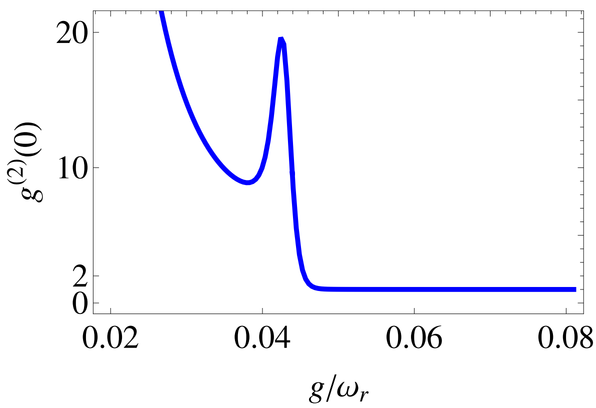

Figure 2. The normalized steady-state second-order photon-photon correlation function $g^{(2)}(0)$ versus the ratio g/ω_r. Other parameters are as in Figure 1.

We proceed further by describing the corresponding quantum dynamics versus the experimentally controllable DQD energy separation ϵ, while all other parameters are being fixed. The resonator-DQD coupling strength g will be selected below or above the threshold, see Figure 1(a) and Figure 1(b), respectively. Thus, Figure 3(a) depicts the mean cavity photon number in these situations. Particularly, near resonance condition, i.e. when $\Omega \approx 2\omega_r$, one can observe a plateau where the mean cavity photon number varies not much, while the scaled energy separation ϵ/ω_r is scanned around the resonance. Then it drops to zero out of the resonance. Above the threshold, i.e. when $g/\omega_r = 0.06$, the current again follows the resonator mean photon number, see Figure 3(b). However, this is not longer the case below the threshold, that is when $g/\omega_r = 0.04$, compare the insets in Figure 3(a) and Figure 3(b), respectively. Furthermore, within the plateau region, the photon statistics is a Poissonian one, since $g^{(2)}(0) \approx 1$, see Figure (4) above the threshold. On the other side, below the threshold condition, the photon statistics is highly super-Poissonian, see the inset in Figure (4). So, one has stable single-qubit lasing effects above the critical value of the cavity-DQD coupling strength, that is, above the threshold.

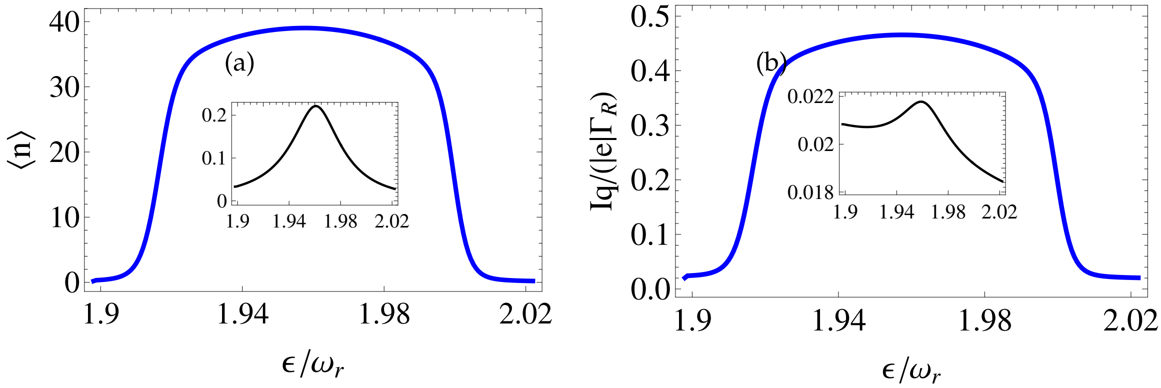

Figure 3. The steady-state behaviours of (a) the mean cavity photon number $\langle n\rangle = \langle a^\dagger a\rangle$ and (b) the current I_q through the DQD system, as a function of ϵ/ω_r. Here $\tau/\omega_r = 0.196$ and $g/\omega_r = 0.06$, while the inset depicts the case when $g/\omega_r = 0.04$, i.e. below the threshold. Other parameters are as in Figure 1.

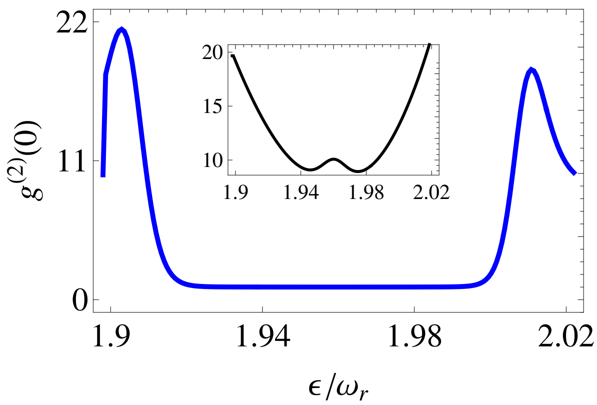

Figure 4. The normalized steady-state second-order photon-photon correlation function $g^{(2)}(0)$ versus the ratio ϵ/ω_r. Other parameters are as in Figure (3).

5. Summary

Summarizing, we have investigated a semiconducting DQD qubit coupled in two-photon resonance with a leaking microwave resonator where the pumping of the qubit is achieved via the environmental electronic reservoirs. Particularly, the inter-dot Coulomb interaction is assumed weak, while the focus is on calculating the mean photon cavity number, under the secular approximation, with a corresponding accent on an obtained critical value for the qubit-resonator coupling strength where the steady-state photon number changes abruptly. Moreover, the corresponding photon statistics vary from super-Poissonian to Poissonian photon statistics. Also, the electric current through the DQD system follows the cavity-mode steady-state photon number behaviours, particularly, above the threshold. This way, one achieves lasing effects in microwave frequency domains, while converting electric current in a photon flux. Respectively, one can estimate the intensity of the photon flux, generated in the cavity mode, via measuring the electric current, or conversely.

Acknowledgments: We highly appreciate the financial support from the Romanian Ministry of Research, Innovation and Digitization, CNCS-UEFISCDI, via the PN-IV-P8-8.3-ROMD-2023-0013 research grant, within PNCDI IV. MM is grateful for the nice hospitality of the Department of Theoretical Physics at the Horia Hulubei National Institute of Physics and Nuclear Engineering as well as for partial support from the Moldavian Ministry of Education and Research, through grant No. 011205.

References

1. Bruhat, L. E.; Cubaynes, T.; Viennot, J. J.; Dartiailh, M. C.; Desjardins, M. M.; Cottet, A.; Kontos, T. Circuit QED with a quantum-dot charge qubit dressed by Cooper pairs, *Phys. Rev. B* **2018**, 98, 155313.
2. Burkard, G.; Gullans, M. J.; Mi, X.; Petta, J. R. Superconductor-semiconductor hybrid-circuit quantum electrodynamics, *Nat. Rev. Phys.* **2020**, 2, 129-140.
3. Haldar, S.; Barker, D.; Havir, H.; Ranni, A.; Lehmann, S.; Dick, K. A.; Maisi, V. F. Continuous Microwave Photon Counting by Semiconductor-Superconductor Hybrids, *Phys. Rev. Lett.* **2024**, 133, 217001.
4. Stanisavljević, O.; . Philippe, J.-C; Gabelli, J.; Aprili, M.; Estéve, J.; Basset, J. Efficient Microwave Photon-to-Electron Conversion in a High-Impedance Quantum Circuit, *Phys. Rev. Lett.* **2024**, 133, 076302.
5. de Sá Neto, O.P.; de Oliveira, M.C. Signal, detection and estimation using a hybrid quantum circuit, *Sci. Rep.* **2024**, 14, 15225.
6. Brandes, T. Coherent and collective quantum optical effects in mesoscopic systems, *Phys. Rep.* **2005**, 408, 315.
7. Kulkarni, M.; Cotlet, O.; Türeci, H. E. Cavity-coupled double-quantum dot at finite bias: analogy with lasers and beyond, *Phys. Rev. B* **2014**, 90, 125402.
8. Liu, Y.-Y.; Stehlik, J.; Eichler, C.; Mi, X.; Hartke, T. R.; Gullans, M. J.; Taylor, J. M.; Petta, J. R. Threshold Dynamics of a Semiconductor Single Atom Maser, *Phys. Rev. Lett.* **2017**, 119, 097702.
9. Tabatabaei, S. M.; Neda, J. Lasing in a coupled hybrid double quantum dot-resonator system, *Phys. Rev. B* **2020**, 101, 115135.
10. Gu, X.; Kockum, A.F.; Miranowicz, A.; Liu, Y.X.; Nori, F. Microwave photonics with superconducting quantum circuits. *Phys. Rep.* **2017**, 1, 718–719.
11. Scarlino, P.; van Woerkom, D. J.; Stockklauser, A.; Koski, J. V.; Collodo, M. C.; Gasparinetti, S.; Reichl, C.; Wegscheider, W.; Ihn, T.; Ensslin, K.; Wallraff, A. All-Microwave Control and Dispersive Readout of Gate-Defined Quantum Dot Qubits in Circuit Quantum Electrodynamics, *Phys. Rev. Lett.* **2019**, 122, 206802.
12. Khan, W.; Potts, P. P.; Lehmann, S.; Thelander, C.; Dick, K. A.; Samuelsson, P.; Maisi, V. F. Efficient and continuous microwave photoconversion in hybrid cavity-semiconductor nanowire double quantum dot diodes, *Nat. Commun.* **2021**, 12, 5130.
13. Havir, H.; Haldar, S.; Khan, W. ; Lehmann, S.; Dick, K. A.; Thelander, C.; Samuelsson, P.; Maisi, V. F. Quantum dot source-drain transport response at microwave frequencies, *Phys. Rev. B* **2023**, 108, 205417.
14. Nian, L.-L.; Hu, S.; Xiong, L.; Lü, J.-T.; Zheng, B. Photon-assisted electron transport across a quantum phase transition, *Phys. Rev. B* **2023**, 108, 085430.
15. Wallraff, A.; Schuster, D. I.; Blais, A.; Frunzio, L.; Huang, R.- S.; Majer, J.; Kumar, S.; Girvin, S. M.; Schoelkopf, R. J. Strong coupling of a single photon to a superconducting qubit using circuit quantum electrodynamics, *Nature* **2004**, 431, 162.
16. Stockklauser, A.; Scarlino, P.; Koski, J. V.; Gasparinetti, S.; Andersen, C. K.; Reichl, C.; Wegscheider, W.; Ihn, T.; Ensslin, K.; Wallraff, A. Strong Coupling Cavity QED with Gate-Defined Double Quantum Dots Enabled by a High Impedance Resonator, *Phys. Rev. X* **2017**, 7, 011030.
17. Gu, S.-S.; Kohler, S.; Xu, Y.-Q.; Wu, R.; Jiang, Sh.-L.; Ye, Sh.-K.; Lin, T.; Wang, B.-Ch.; Li, H.-O. Probing Two Driven Double Quantum Dots Strongly Coupled to a Cavity, *Phys. Rev. Lett.* **2023**, 130, 233602.
18. Ungerer, J. H.; Pally, A.; Kononov, A.; Lehmann, S.; Ridderbos, J.; Potts, P. P.; Thelander, C.; Dick, K. A.; Maisi, V. F.; Scarlino, P.; Baumgartner, A.; Schönenberger, C. Strong coupling between a microwave photon and a singlet-triplet qubit, *Nat. Commun.* **2024**, 15, 1068.
19. Wong, C. H.; Vavilov, M. G. Quantum efficiency of a single microwave photon detector based on a semiconductor double quantum dot, *Phys. Rev. A* **2017**, 95, 012325.
20. Ghirri, A.; Cornia, S.; Affronte, M. Microwave photon detectors based on semiconducting double quantum dots, *Sensors* **2020**, 20, 4010.

21. Nian, L.-L.; Zheng, B.; Lü, J.-T. Electrically driven photon statistics engineering in quantum-dot circuit quantum electrodynamics, *Phys. Rev. B* **2023**, 107, L241405.
22. Brandes, T. Coherent and collective quantum optical effects in mesoscopic systems, *Phys. Rep.* **2005**, 408, 315.
23. Sánchez, R.; Platero, G.; Brandes, T. Resonance Fluorescence in Transport through Quantum Dots: Noise Properties, *Phys. Rev. Lett.* **2007**, 98,146805.
24. Xu, C.; Vavilov, M. G. Full counting statistics of photons emitted by a double quantum dot, *Phys. Rev. B* **2013**, 88, 195307.
25. Agarwalla, B. K.; Kulkarni, M.; Mukamel, S.; Segal, D. Tunable photonic cavity coupled to a voltage-biased double quantum dot system: Diagrammatic nonequilibrium Green's function approach, *Phys. Rev. B* **2016**, 94, 035434.
26. Chen, C.-C.; Stace, T. M.; Goan, H.-S. Full-polaron master equation approach to dynamical steady states of a driven two-level system beyond the weak system-environment coupling, *Phys. Rev. B* **2020**, 102, 035306.
27. Hazra, S. K.; Addepalli, L.; Pathak, P. K.; Dey, T. N. Nondegenerate two-photon lasing in a single quantum dot, *Phys. Rev. B* **2024**, 109, 155428.
28. Jin, J.; Marthaler, M.; Jin, P.-Q.; Golubev, D.; Schön, G. Noise spectrum of a quantum dot-resonator lasing circuit, *New J. Phys.* **2013**, 15, 025044.
29. Lambert, N.; Flindt, C.; Nori, F. Photon-mediated electron transport in hybrid circuit-QED, *EPL* **2013**, 103, 17005.
30. Shi, P.; Hu, M.; Ying, Y.; Jin, J. Noise spectrum of quantum transport through double quantum dots: Renormalization and non-Markovian effects, *AIP Advances* **2016**, 6, 095002.
31. Karlewski, C.; Heimes, A.; Schön, G. Lasing and transport in a multilevel double quantum dot system coupled to a microwave oscillator, *Phys. Rev. B* **2016**, 93, 045314.
32. Jin, J. Nonequilibirum noise spectrum and Coulomb blockade assisted Rabi interference in a double-dot Aharonov-Bohm interferometer, *Phys. Rev. B* **2020**, 101, 235144.
33. Drummond P. D.; Walls, D. F. Quantum theory of optical bistability. I. Nonlinear polarisability model, *J. Phys. A* **1980**, 13, 725.
34. Macovei, M. A. Measuring photon-photon interactions via photon detection, *Phys. Rev. A* **2010**, 82, 063815.
35. Zenelaj, D.; Potts, P. P.; Samuelsson, P. Full counting statistics of the photocurrent through a double quantum dot embedded in a driven microwave resonator, *Phys. Rev. B* **2022**, 106, 205135.
36. Zenelaj, D.; Samuelsson, P.; Potts, P. P. Wigner-function formalism for the detection of single microwave pulses in a resonator-coupled double quantum dot, *Phys. Rev. Research* **2025**, 7, 013305.
37. Jin, P.-Q.; Marthaler, M.; Cole, J. H.; Shnirman, A.; Schön, G. Lasing and transport in a quantum-dot resonator circuit, *Phys. Rev. B* **2011**, 84, 035322.
38. Rastelli, G.; Governale, M. Single atom laser in normal-superconductor quantum dots, *Phys. Rev. B* **2019**, 100, 085435.
39. Mantovani, M.; Armour, A. D.; Belzig, W.; Rastelli, G. Dynamical multistability in a quantum-dot laser, *Phys. Rev. B* **2019**, 99, 045442.
40. Agarwalla, B. K.; Kulkarni, M.; Segal, D. Photon statistics of a double quantum dot micromaser: Quantum treatment, *Phys. Rev. B* **2019**, 100, 035412.
41. Tabatabaei, S. M.; Jahangiri, N. Lasing in a coupled hybrid double quantum dot-resonator system, *Phys. Rev. B* **2020**, 101, 115135.
42. Stace, T. M.; Doherty, A. C.; Barrett, S. D. Population Inversion of a Driven Two-Level System in a Structureless Bath, *Phys. Rev. Lett.* **2005**, 95, 106801.
43. Müller, C.; Stace, Th. M. Deriving Lindblad master equations with Keldysh diagrams: Correlated gain and loss in higher order perturbation theory, *Phys. Rev. A* **2017**, 95, 013847.
44. Mihaescu, T.; Isar A.; Macovei, M. A. Two-quanta processes in coupled double-quantum-dot cavity systems, *arXiv:2501.05967v1* **2025**.
45. Nian, L.-L.; Wang, Y.-Ch.; Wang, J.-Y.; Xiong, L.; Zheng, B.; Lü, J.-T. Dissipative quantum phase transitions in electrically driven lasers, *arXiv:2501.10997v2* **2025**.
46. Agarwal, G. S. *Quantum Statistical Theories of Spontaneous Emission and their Relation to Other Approaches* , Springer, Berlin, 1974.
47. Kiffner, M.; Macovei, M.; Evers, J.; Keitel, C. H. Vacuum induced processes in multilevel atoms, *Prog. Opt.* **2010**, 55, 85.
48. James, D. F. V. Quantum Computation with Hot and Cold Ions: An Assessment of Proposed Schemes, *Fort. Phys.* **2000**, 48, 823.

 doi:10.20944/preprints202508.1322.v1

49. Tan, R. ; Li, G.-X.; Ficek, Z. Squeezed single-atom laser in a photonic crystal, *Phys. Rev. A* **2008**, 78, 023833.
50. Quang, T.; Freedhoff, H. Atomic population inversion and enhancement of resonance fluorescence in a cavity, *Phys. Rev. A* **1993**, 47, 2285.
51. Mihaescu, T.; Cecoi, E.; Macovei, M. A.; Isar, A. Geometric discord for a driven two-qubit system, *Rom. Rep. Phys.* **2021**, 73, 101.
52. Glauber, R. J. The Quantum Theory of Optical Coherence, *Phys. Rev.* **1963**, 130, 2529.